Inorg. Chem. **1985**, *24*, 4055–4062 **4055**

Contribution from the Department of Chemistry, Columbia University, New York, New York 10027,
Department of Chemistry, University of Nebraska, Lincoln, Nebraska 68588,
and School of Chemical Sciences, University of Illinois, Urbana, Illinois 61801

Synthesis and Structure of the $[(\eta^5\text{-}C_5H_5)Ti(Mo_5O_{18})]^{3-}$ and $[(\eta^5\text{-}C_5H_5)Ti(W_5O_{18})]^{3-}$ Anions

T. M. CHE,[1a] V. W. DAY,*[1b] L. C. FRANCESCONI,[1a,c] M. F. FREDRICH,[1b] W. G. KLEMPERER,*[1a,c] and W. SHUM[1a]

Received January 30, 1985

Stoichiometric quantities of $(Mo_2O_7)[(n\text{-}C_4H_9)_4N]_2$, $(C_5H_5)_2TiCl_2$, and water react in CH_2Cl_2 solution to form $[(\eta^5\text{-}C_5H_5)Ti(Mo_5O_{18})][(n\text{-}C_4H_9)_4N]_3$ (**1**). The tungsten analogue, $[(\eta^5\text{-}C_5H_5)Ti(W_5O_{18})][(n\text{-}C_4H_9)_4N]_3$ (**2**), is formed in a similar fashion from stoichiometric quantities of $(WO_4)[(n\text{-}C_4H_9)_4N]_2$, $(C_5H_5)_2TiCl_2$, and aqueous HCl in CH_3CN. According to IR and ^{17}O NMR spectroscopy, anions **1** and **2** are isostructural and are related to the octahedral $M^{VI}{}_6O_{19}{}^{2-}$ anions, M = Mo, W, by substitution of $[M^{VI}O]^{4+}$ units with $[Ti^{IV}(C_5H_5)]^{3+}$ units. Comparison of structural parameters for anion **1**, obtained from a single-crystal X-ray diffraction study [$a = 25.162$ (9) Å, $c = 50.380$ (10) Å, $Z = 16$, space group $I4_1cd\text{-}C_{4v}^{12}$], with known structural parameters for the parent $Mo_6O_{19}{}^{2-}$ anion reveals a pattern of trans bond length alternation resulting from the metal center substitution. This bond length alternation provides a mechanism for surface charge delocalization.

Introduction

A large family of Mo^{VI} and W^{VI} polyoxoanion structures is based on neutral $M^{VI}{}_nO_{3n}$ cages that encapsulate one or more central, anionic subunits.[2] Each hexavalent metal center in these cages has the local oxygen environment shown in A. Here, a double line represents a 1.6–1.7-Å metal–oxygen double bond, a single line a 1.8–2.1-Å metal–oxygen single[3] bond, and a dotted line a very weak, >2.2-Å metal–oxygen bond. The $M^{VI}O_t$ units are linked together by doubly bridging O_b oxygens to form a cage, and the O_c oxygen is part of a central, anionic subunit. The simplest members of this structural family are the octahedral $Mo^{VI}{}_6O_{19}{}^{2-}$ [4] and $W^{VI}{}_6O_{19}{}^{2-}$ [5] anions, whose structures are based on an $M^{VI}{}_6O_{18}$ cage encapsulating a central O^{2-} unit (B).

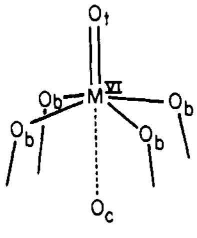

A

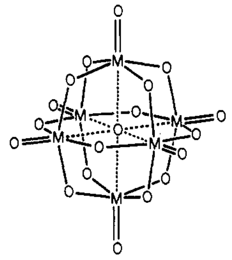

B

As might be expected from the bonding scheme A, the O_t and O_b oxygens that constitute the $M^{VI}{}_nO_{3n}$ cage surfaces are quite nonbasic and unreactive.[6] They can be activated, however, by replacing the hexavalent cage metal centers with one or more lower valent metals. In the simplest $M^{VI}{}_6O_{19}{}^{2-}$ case, for example, *cis*-$V^V{}_2W^{VI}{}_4O_{19}{}^{4-}$ is readily protonated,[7] and the *cis*-$Nb^V{}_2W^{VI}{}_4O_{19}{}^{4-}$ anion forms stable adducts with cations such as $[(OC)_3Mn]^+$,[8] $\{[(CH_3)_5C_5]Rh\}^{2+}$,[9] $[(C_7H_8)Rh]^+$,[10] H^+,[11] $CH_3{}^+$,[11] and $[(CH_3)_3Si]^+$.[11] This mode of surface activation, however, can present several problems. First, the activated polyoxoanions tend to disorder in the solid state since the penta- and hexavalent cage metals are separated from the cage's exterior environment by a symmetric shell of O_b and O_t oxygens and the anions can disorder according to this pseudosymmetry.[12] As a result, structural parameters are available only for the disorder-averaged species and detailed structure–reactivity correlations have been difficult to establish. A second problem, related in part to this pseudosymmetry, is a tendency of the activated polyoxoanions to form mixtures of permutational isomers upon adduct formation. The solvated $[(OC)_3Mn]^+$ [8] and $\{[(CH_3)_5C_5]Rh\}^{2+}$ [9] cations each react with *cis*-$Nb_2W_4O_{19}{}^{4-}$, for example, to form a mixture of three diastereomers. A final problem is the potentially nonselective nature of this surface activation, which can result in activation of both the terminal (O_t) and bridging (O_b) surface oxygens (C).

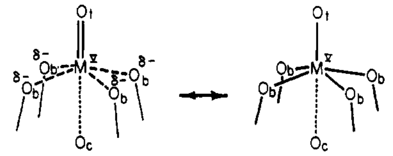

C

---

(1) (a) Columbia University. (b) University of Nebraska. (c) University of Illinois (current address).

(2) Day, V. W.; Klemperer, W. G. *Science (Washington, D.C.)* **1985**, *228*, 533–41.

(3) We refer to bond strength in the electrostatic sense, not bond order in the molecular orbital sense. For bond strength–bond length correlations see: (a) Kihlborg, L. *Ark. Kemi* **1963**, *21*, 471–95. (b) Allmann, R. *Monatsh. Chem.* **1975**, *106*, 779–93. (c) Schroeder, F. A. *Acta Crystallogr., Sect. B: Struct. Crystallogr. Cryst. Chem.* **1975**, *B31*, 2294–309. (d) Brown, I. D.; Wu, K. K. *Acta Crystallogr., Sect. B: Struct. Crystallogr. Cryst. Chem.* **1976**, *B32*, 1957–9.

(4) (a) Allcock, H. R.; Bissell, E. C.; Shawl, E. T. *Inorg. Chem.* **1973**, *12*, 2963–8. (b) Garner, C. D.; Howlader, N. C.; Mabbs, F. E.; McPhail, A. T.; Miller, R. W.; Onan, K. D. *J. Chem. Soc., Dalton Trans.* **1978**, 1582–9. (c) Nagano, O.; Sasaki, Y. *Acta Crystallogr., Sect. B: Struct. Crystallogr. Cryst. Chem.* **1979**, *B35*, 2387–9.

(5) (a) Henning, G.; Huellen, A. *Z. Kristallogr., Kristallgeom., Kristallphys., Kristallchem.* **1969**, *130*, 162–72. (b) Kirillova, N. I.; Kolomnikov, I. S.; Zolotarev, Yu. A.; Lysyak, T. V.; Struchkov, Yu. T. *Soviet J. Coord. Chem. (Engl. Transl.)* **1978**, *B34*, 1764–70. (c) Fuchs, J.; Freiwald, W.; Hartl, H. *Acta Crystallogr., Sect. B: Struct. Crystallogr. Cryst. Chem.* **1978**, *B34*, 1764–70. (d) LaRue, W. A.; Liu, A. T.; San Filippo, J., Jr. *Inorg. Chem.* **1980**, *19*, 315–20.

(6) A quantitative measure of low surface charge density is provided by heteroconjugation studies, which indicate, for example, that $Mo_6O_{19}{}^{2-}$ and $ClO_4{}^-$ have comparable hydrogen bond accepting abilities: Barcza, L.; Pope, M. T. *J. Phys. Chem.* **1975**, *79*, 92–3.

(7) Klemperer, W. G.; Shum, W. *J. Am. Chem. Soc.* **1978**, *100*, 4891–3.

(8) (a) Besecker, C. J.; Day, V. W.; Klemperer, W. G.; Thompson, M. R. *Inorg. Chem.* **1985**, *24*, 44–50. (b) Besecker, C. J.; Klemperer, W. G. *J. Am. Chem. Soc.* **1980**, *102*, 7598–7600.

(9) Besecker, C. J.; Day, V. W.; Klemperer, W. G.; Thompson, M. R. *J. Am. Chem. Soc.* **1984**, *106*, 4125–36.

(10) Besecker, C. J.; Klemperer, W. G.; Day, V. W. *J. Am. Chem. Soc.* **1982**, *104*, 6158–9.

(11) Day, V. W.; Klemperer, W. G.; Schwartz, C., manuscript in preparation.

(12) (a) Botar, A.; Fuchs, J. *Z. Naturforsch., B: Anorg. Chem.; Org. Chem.* **1982**, *37B*, 806–14. (b) Nishikawa, K.; Kobayashi, A.; Sasaki, Y. *Bull. Chem. Soc. Jpn.* **1975**, *48*, 889–92.

0020-1669/85/1324-4055$01.50/0 © 1985 American Chemical Society

In the $\{[(C_7H_8)Rh]_5(Nb_2W_4O_{19})_2\}^{3-}$ anion, for example, Rh^I centers are bound to both O_t and O_b oxygens.[10]

One solution to the problems just mentioned is activation of $M^{VI}{}_6O_{19}{}^{2-}$ surfaces not by replacement of M^{VI} centers with M^V centers but by replacement of entire $M^{VI}O_t{}^{4+}$ units by $[Ti^{IV}(\eta^5\text{-}C_5H_5)]^{3+}$ units (D). This substitution addresses the problems raised above by (a) introducing an external cage substituent at the metal substitution site that tends to eliminate disorder in crystal packing, (b) introducing a relatively bulky cyclopentadienyl group that sterically shields adjacent O_b oxygens and thus reduces the potential for isomerism in adduct anions, and (c) introducing a structural unit that does not contain a terminal oxygen and therefore tends to activate O_b oxygens selectively (compare C and D). In this paper we describe the synthesis and characterization of the two simplest $M^{VI}{}_6O_{19}{}^{2-}$ derivatives that have been activated in this manner, the $[(\eta^5\text{-}C_5H_5)Ti(Mo_5O_{18})]^{3-}$[13] and $[(\eta^5\text{-}C_5H_5)Ti(W_5O_{18})]^{3-}$ anions. In addition, we present detailed solid-state structural data for the molybdenum complex that in conjunction with ^{17}O NMR spectroscopic data provide insight into the mechanism of surface activation and charge delocalization in these and related species. The reaction chemistry of the title complexes will be described in future publications.

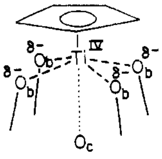

D

Experimental Section

Reagents, Solvents, and General Procedures. The following were purchased from commercial sources and used without further purification: 0.4 M aqueous tetra-*n*-butylammonium hydroxide (Eastman), 1 M methanolic tetra-*n*-butylammonium hydroxide (Eastman), tungsten trioxide monohydrate (Baker), concentrated HCl (Mallinckrodt), ^{17}O-enriched water (Monsanto Research), acetone (Fisher), anhydrous diethyl ether (Baker), CD_3CN (Merck), and CD_2Cl_2 (Merck). $(C_5H_5)_2TiCl_2$ (Pressure Chemical) was recrystallized once by cooling a saturated 40 °C CH_2Cl_2 solution to 0 °C. The precise concentration of aqueous $(n\text{-}C_4H_9)_4NOH$ was determined by titration with 0.10 N HCl to a phenolphthalein endpoint. Procedures described in ref 14 were followed for the preparation of $(\alpha\text{-}Mo_8O_{26})[(n\text{-}C_4H_9)_4N]_4$. Methylene chloride (Baker) was distilled once from P_4O_{10}, and acetonitrile (Aldrich, 99%) was distilled twice, once from P_4O_{10} and once from CaH_2. *n*-Propyl alcohol was also distilled twice, from K_2CO_3 and then from CaH_2. Toluene (MCB) was distilled from sodium-benzophenone ketyl under dinitrogen.

Analytical Procedures. Elemental analyses were performed by Galbraith Laboratories, Knoxville, TN, and by the School of Chemical Sciences Microanalytical Laboratory at the University of Illinois.

Infrared spectra were recorded from KBr pellets with a Perkin-Elmer Model 621 spectrometer and were referenced to the 1028-cm^{-1} band of a 0.5-mm polystyrene film. Absorptions are described below as follows: very strong (vs), strong (s), medium (m), shoulder (sh), and broad (br).

^1H NMR spectra were recorded on Perkin-Elmer R32 (90 MHz) and Nicolet NT-360 (360 MHz) spectrometers and referenced internally to $(CH_3)_4Si$. ^{17}O FTNMR spectra were measured at 13.51 MHz in 10-mm sample tubes with a JEOL PFT/PS-100 spectrometer interfaced with a Nicolet 1080 data system and at 33.93 MHz in 12-mm sample tubes with a spectrometer equipped with a 5.87-T Oxford Instruments magnet and a Nicolet NIC-80 data system and referenced externally to pure H_2O at 25 °C. Chemical shifts for all nuclei are reported as positive values for resonances that are observed at higher frequency (lower field) than the appropriate reference.

Preparation of $(Mo_2O_7)[(n\text{-}C_4H_9)_4N]_2$. This compound was prepared with use of Liu's modification[15] of a literature procedure.[14] A 100-mL beaker containing a stirring bar was charged with $(\alpha\text{-}Mo_8O_{26})[(n\text{-}C_4H_9)_4N]_4$ (5.0 g, 2.3 mmol), 50 mL of CH_2Cl_2, and 9.5 mL of 1 M methanolic $(n\text{-}C_4H_9)_4NOH$ (9.5 mmol). After 20 min of stirring, almost all of the $(\alpha\text{-}Mo_8O_{26})[(n\text{-}C_4H_9)_4N]_4$ was dissolved, and the solution was filtered to remove small amounts of solid material. The resulting clear solution was then concentrated on a rotary evaporator to a viscous oil. The oil was then dissolved in 10 mL of acetone and stirred for 5 min. Anhydrous diethyl ether (100 mL) was added to this solution, yielding an oil that became crystalline after ca. 1 min of stirring and scraping with a spatula. The solid was collected by filtration, washed with 20 mL of anhydrous diethyl ether, and dried in vacuo for 2 h to give 5.7 g of crude product. Pure product was obtained by dissolving this white powder in 20 mL of acetonitrile, filtering off any insoluble material, and then carefully adding ca. 11 mL of anhydrous ether, without stirring, to produce a saturated solution. Cooling to 0 °C for 10 h induced the formation of large colorless crystals, which were collected by filtration and dried to vacuo to yield 4.4 g of product (5.6 mmol, 61% based on Mo).

Table I. ^{17}O FTNMR Chemical Shifts and Line Widths for $[(\eta^5\text{-}C_5H_5)Ti(Mo_5O_{18})]^{3-}$ (**1**) and $[(\eta^5\text{-}C_5H_5)Ti(W_5O_{18})]^{3-}$ (**2**) as Tetra-*n*-butylammonium Salts in CH_3CN[a]

assignt[b]	**1**[c]	**2**[d]	assignt[b]	**1**[c]	**2**[d]
$OTiM_5$	5 (11)	−62 (18)	OTiM	641 (49)	544 (56)
OM_2	516 (93)	380 (71)	OM	834 (93)	704 (68)
	535 (64)	392 (63)		863 (130)	709 (65)

[a] Spectra shown in Figure 2; chemical shifts in ppm downfield from pure H_2O at 25 °C are accurate ±3 ppm; line widths (fwhm) in Hz, ±15 Hz for **1** and ±5 Hz for **2**, have been corrected for exponential line broadening and are enclosed in parentheses. [b] Oxygen types are identified by the identity and number of metals each oxygen is bonded to, M = Mo for **1** and W for **2** (see Figure 2). [c] Conditions: 25 °C; 0.23 M; 19 atom % ^{17}O; 13.513 MHz; 12 000 acquisitions; 4.9 Hz/data point; 7.7-Hz pulse repetition rate; 11-Hz exponential line broadening. [d] Conditions: 79 °C; 0.01 M; 6 atom % ^{17}O; 33.928 MHz; 218 000 acquisitions; 3.1 Hz/data point; 3-Hz pulse repetition rate; 5-Hz exponential line broadening.

Preparation of $[(\eta^5\text{-}C_5H_5)Ti(Mo_5O_{18})][(n\text{-}C_4H_9)_4N]_3$. This preparation must be carried out in a dinitrogen atmosphere to avoid hydrolysis of the product. A solution of $(C_5H_5)_2TiCl_2$ (0.50 g, 2.0 mmol) in 40 mL of CH_2Cl_2 was added over a ca. 45-min period with rapid stirring to a solution of deionized water (12 μL, 0.67 mmol) and $(Mo_2O_7)[(n\text{-}C_4H_9)_4N]_2$ (4.0 g, 5.1 mmol) in 30 mL of CH_2Cl_2. The reaction was relatively slow, and the rate of $(C_5H_5)_2TiCl_2$ addition was adjusted to match the rate of reaction. This was monitored by observing the color of the reaction solution. Since the product is yellow, the reaction solution took on an orange tint if the red $(C_5H_5)_2TiCl_2$ solution was added too rapidly. Note that the amount of water used (12 μL, 0.67 mmol) was less than the stoichiometric quantity (18 μL, 1.0 mmol), because the dried solvent contained significant amounts of water. The amount of water added may therefore have to be adjusted, depending on drying efficiency. The total amount of water present is critical since excess water decomposes the product and insufficient water leads to a brown discoloration of the reaction solution, arising presumably from reduction of Mo^{VI} by $C_5H_5{}^-$. Once the reaction was complete, ca. 150 mL of toluene was added and the CH_2Cl_2 allowed to slowly evaporate under a slow flow of dinitrogen over a period of 2–3 days. The product separated from the reaction solution during this time period as yellow crystals, which were collected by filtration, washed with 3 × 25 mL of anhydrous diethyl ether, and dried to yield 1.9 g of product (1.2 mmol, 58% based on Mo) as a yellow powder. Anal. Calcd for $C_{53}H_{113}N_3TiMo_5O_{18}$: C, 39.59; H, 7.08; N, 2.61; Ti, 2.98; Mo, 29.83. Found: C, 39.84; H, 7.49; N, 2.52; Ti, 3.16; Mo, 30.28. IR (KBr, 350–1000 cm^{-1}, see Figure 1a): 950 (s), 920 (vs), 822 (w), 795 (vs, br), 775 (vs, sh), 425 (s), 414 (s), 366 (m). ^1H NMR (CD_2Cl_2, 90 MHz): δ 6.13 (s, C_5H_5); 3.2–3.4 (m, NCH_2); 1.3–1.9 (m, $NCH_2CH_2CH_2$); 0.9–1.2 (m, CH_3). ^{17}O NMR: see Table I and Figure 2a.

Material enriched in ^{17}O was prepared under a dry N_2 atmosphere from enriched water and $(Mo_2O_7)[(n\text{-}C_4H_9)_4N]_2$ enriched with use of the procedure described in ref 14. All ^{17}O-enriched molybdates were stored and handled under dry N_2 to avoid isotopic dilution.

Preparation of $(WO_4)[(n\text{-}C_4H_9)_4N]_2$. To a hot (80 °C) solution of 0.35 M aqueous $(n\text{-}C_4H_9)_4NOH$ (487 mL, 170 mmol) was added $WO_3{\cdot}H_2O$ (22 g, 88 mmol) with stirring in ca. 3-g increments over a 5-min period. When the addition was complete, the reaction mixture was stirred for 5–10 min at 80 °C and then cooled to room temperature and filtered to remove undissolved $WO_3{\cdot}H_2O$. The resulting clear solution was then boiled for ca. 1$^1/_2$ h to reduce the volume to 125 mL, and further water was removed on a rotary evaporator under vacuum at 80

---

(13) The synthesis and structure of $[(C_5H_5)Ti(Mo_5O_{18})][(n\text{-}C_4H_9)_4N]_3$ have been reported in preliminary communications: (a) Klemperer, W. G.; Shum, W. *J. Chem. Soc., Chem. Commun.* **1979**, 60–1. (b) Day, V. W.; Fredrich, M. F.; Thompson, M. R.; Klemperer, W. G.; Liu, R.-S.; Shum, W. *J. Am. Chem. Soc.* **1981**, *103*, 3597–9.

(14) Filowitz, M.; Ho, R. K. C.; Klemperer, W. G.; Shum, W. *Inorg. Chem.* **1979**, *18*, 93–103.

(15) Liu, R.-S. Ph.D. Dissertation, Columbia University, New York, 1980.

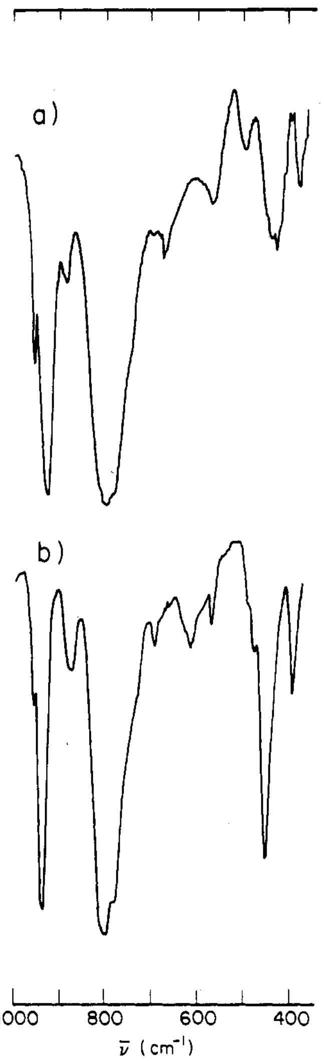

Figure 1. IR spectra of (a) $[(\eta^5\text{-}C_5H_5)Ti(Mo_5O_{18})][(n\text{-}C_4H_9)_4N]_3$ and (b) $[(\eta^5\text{-}C_5H_5)Ti(W_5O_{18})][(n\text{-}C_4H_9)_4N]_3$ measured from KBr pellets. See Experimental Section for numerical data.

°C to obtain a moist white solid. This material was thoroughly dried in a vacuum at 60 °C for 24 h. During the drying process, the solid was ground to a powder under a dry dinitrogen atmosphere three times, after ca. 3, 6, and 15 h of drying. The yield was 52 g (71 mmol, 84% based on $(n\text{-}C_4H_9)_4NOH$). This material is extremely hygroscopic and must be stored in a desiccator. Anal. Calcd for $C_{32}H_{72}N_2WO_4$: C, 52.45; H, 9.90; N, 3.82; W, 25.09. Found: C, 52.54; H, 10.05; N, 3.97; W, 24.91.

Preparation of $[(\eta^5\text{-}C_5H_5)Ti(W_5O_{18})][(n\text{-}C_4H_9)_4N]_3$. Aqueous HCl (0.80 M, 17 mL, 14 mmol) and then a solution of $(C_5H_5)_2TiCl_2$ (0.68 g, 2.7 mmol) in 20 mL of CH_2Cl_2 were added rapidly, with vigorous stirring, to a solution of $(WO_4)[(n\text{-}C_4H_9)_4N]_2$ (10 g, 14 mmol) in 60 mL of acetonitrile. The resulting solution turned from a bright red color to a yellow color after ca. 10 min of rapid stirring and was then stirred for a further 10 min, after which solvents were removed under reduced pressure on a rotary evaporator to yield ca. 10 mL of a yellow oil containing some white powder. Crude product was isolated from this suspension by performing a series of four precipitations from *n*-propyl alcohol as follows. The suspension was diluted with 10 mL of *n*-propyl alcohol and then poured into 200 mL of diethyl ether with vigorous stirring. The resulting mixture was stirred for ca. 5 min and then allowed to sit undisturbed for ca. 20 min, after which ether, which formed a separate layer, was decanted. After each successive precipitation, the material remaining contained less oil and more solid until after the fourth precipitation only white solid remained. This material was washed with 30 mL of diethyl ether, isolated by suction filtration, and dried in vacuo to give 4.3 g of crude product. To obtain pure, crystalline product, this solid was placed into a 400-mL beaker containing 200 mL of *n*-propyl alcohol. The resulting suspension was heated to boiling with stirring and then allowed to cool to room temperature without stirring. After 10 h, the suspension was filtered to remove ca. 1.2 g of white solid and the filtrate concentrated to 50 mL by boiling off solvent. The solution obtained was allowed to cool to room temperature and was filtered a second time to remove a trace amount of white solid. This filtrate was then concentrated to 25 mL, and after it was cooled to room temperature, small, clear, colorless, block-shaped crystals appeared within 2 h. After 24 h, crystals were collected by suction filtration and washed quickly with ca. 10 mL of cold *n*-propyl alcohol and then ca. 20 mL of diethyl ether. A second crop was obtained by combining the 10-mL *n*-propyl alcohol wash with the mother liquor, reducing the volume to ca. 5 mL by boiling off solvent, and isolating crystals as just described for the first crop. In order to obtain product completely free of *n*-propyl alcohol, it was necessary to keep the product under vacuum at 60 °C for 24 h. The first and second crops produced 1.2 and 1.0 g of material, respectively, yielding a total of 2.2 g (1.1 mmol, 39% based on tungsten) of product as a white powder. One further crystallization was performed for the microanalytical sample only. Anal. Calcd for $C_{53}H_{113}N_3TiW_5O_{18}$: C, 31.09; H, 5.56; N, 2.05; Ti, 2.34; W, 44.89. Found: C, 30.85; H, 5.48; N, 2.01; Ti, 2.13; W, 44.63. IR (KBr, 350–1000 cm^{-1}): 962 (m), 942 (vs), 882 (m), 805 (vs), 782 (sh), 436 (s), 380 (m). ^1H NMR (CD_3CN, 360 MHz): δ 6.04 (s, 5, C_5H_5), 3.14 (m, 24, NCH_2), 1.63 (m, 24, $NCH_2CH_2CH_2CH_3$), 1.38 (m, 24, $NCH_2CH_2CH_2CH_3$), 0.98 (m, 36, CH_3). ^{17}O NMR: see Table I and Figure 2b.

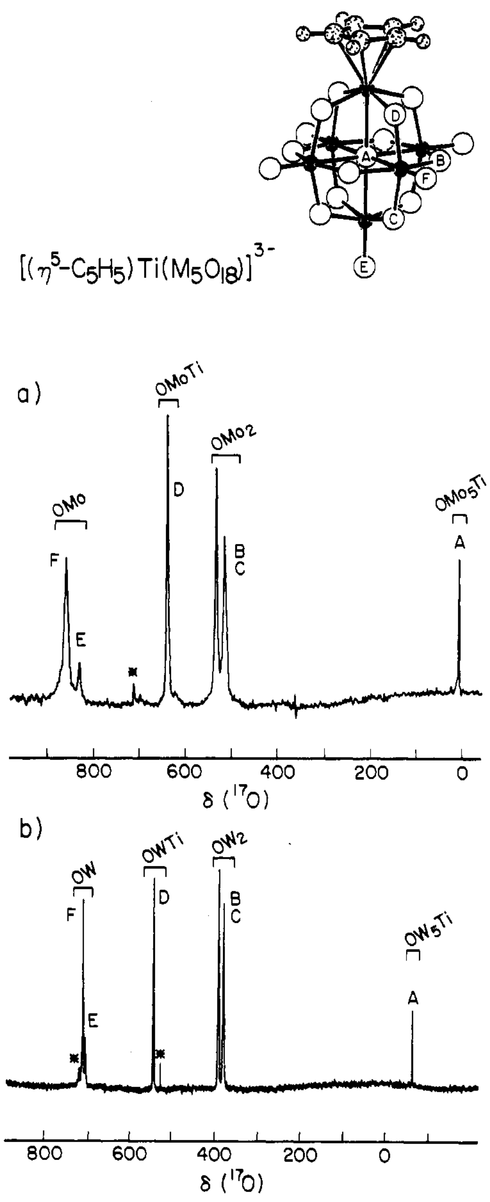

Figure 2. ^{17}O NMR spectra of (a) $[(\eta^5\text{-}C_5H_5)Ti(Mo_5O_{18})][(n\text{-}C_4H_9)N]_3$ and (b) $[(\eta^5\text{-}C_5H_5)Ti(W_5O_{18})][(n\text{-}C_4H_9)_4N]_3$. See Table II for numerical data and spectral parameters. Resonances are assigned with use of the oxygen labeling scheme indicated in the SCHAKAL drawing. Asterisks identify resonances arising from sample decomposition, in (a), and from contamination, in (b).

Material enriched in ^{17}O to 6% was prepared from 6% ^{17}O-enriched aqueous HCl and $(WO_4)[(n\text{-}C_4H_9)_4N]_2$ enriched in ^{17}O to 6% by stirring 10 g (13.7 mmol) of material in 1.2 mL of 11.2% ^{17}O-enriched water for

1 h. The enriched water was then degassed on a vacuum line and recovered by distillation at room temperature into a receiving flask maintained at liquid-nitrogen temperature. The initial phases of the preparation, up to removal of reaction solvent on a rotary evaporator, were carried out under dry N_2 to avoid isotopic dilution.

X-ray Crystallographic Study[16] of $[(\eta^5\text{-}C_5H_5)Ti(Mo_5O_{18})][(n\text{-}C_4H_9)_4N]_3$ (1). Large, well-shaped yellow single crystals of the CH_2Cl_2 solvate of $[(\eta^5\text{-}C_5H_5)Ti(Mo_5O_{18})][(n\text{-}C_4H_9)_4N]_3$ (**1**) suitable for x-ray diffraction studies were obtained as described above. They are, at 20 ± 1 °C, tetragonal with $a = 25.162$ (9) Å, $c = 50.380$ (10) Å, $V = 31897$ Å^3, and $Z = 16$ (μ_a(Mo K$\bar{\alpha}$)[17a] = 0.96 mm^{-1}; $d_{calcd} = 1.410$ g cm^{-3}). The systematically absent reflections in the diffraction pattern were those for the uniquely determined noncentrosymmetric space group $I4_1cd\text{-}C_{4v}^{12}$ (No. 110).[18]

Intensity measurements were made on a Nicolet P$\bar{1}$ autodiffractometer using 1.0°-wide ω scans and graphite-monochromated Mo K$\bar{\alpha}$ radiation for an approximately cube-shaped specimen 0.58 mm on an edge. This crystal was sealed with mother liquor inside a thin-walled glass capillary and mounted on the goniometer head with an edge nearly parallel to the ϕ axis of the diffractometer. A total of 7412 independent reflections having $2\theta_{\text{Mo K}\bar{\alpha}} < 50.7°$ (the equivalent of 0.80 limiting Cu K$\bar{\alpha}$ spheres) were measured in two concentric shells of increasing 2θ. A scanning rate of 3°/min was used to measure intensities for reflections having $3° < 2\theta < 43.0°$ and a rate of 2°/min was used for all others. Each of these 1.0°-wide scans was divided into 19 equal (time) intervals, and those 13 contiguous intervals that had the highest single accumulated count at their midpoint were used to calculate the net intensity from scanning. Background counts, each lasting for one-fourth the total time used for the net scan ($^{13}/_{19}$ of the total scan time), were measured at ω settings 1.0° above and below the calculated K$\bar{\alpha}$ doublet value for each reflection. The linear absorption coefficient of the crystal for Mo K$\bar{\alpha}$ radiation is 0.96 mm^{-1}, yielding a μR value of 0.344 for a spherical crystal having the same volume as the cube-shaped specimen used for intensity measurements. The absorption of X-rays by a spherical crystal having $\mu R = 0.344$ is virtually independent of scattering angle,[19] and deviations from this absorption occasioned by the use of the cube-shaped specimen are practically negligible except for a trivial fraction of the reflections. Under these circumstances, no absorption correction was made and the intensities were reduced to a set of relative squared amplitudes, $|F_o|^2$, by means of appropriate Lorentz and polarization corrections.

The structure was solved with use of statistical "direct methods" techniques (MULTAN). Unit-weighted full-matrix least-squares refinement which utilized anisotropic thermal parameters for all non-hydrogen atoms of the anion and isotropic thermal parameters for non-hydrogen atoms of the cations converged to R_1 (unweighted, based on F)[20] = 0.060 and R_2 (weighted, based on F)[20] = 0.071 for 2556 independent reflections having $2\theta_{\text{Mo K}\bar{\alpha}} \leqslant 43°$ and $I > 3\sigma(I)$. A difference Fourier synthesis calculated at this point revealed the three non-hydrogen atoms of the CH_2Cl_2 solvent molecule of crystallization but few chemically reasonable positions for hydrogen atoms. These three solvent non-hydrogen atoms and idealized cyclopentadienyl hydrogen atoms[21] were included in the structural model for all subsequent least-squares refinement cycles. Additional cycles of unit-weighted full-matrix least-squares refinement which employed the more complete ($2\theta_{\text{Mo K}\bar{\alpha}} < 50.7°$) data set, a least-squares refinable extinction correction[22] of the form $1/(1 + 2gI_c)^{1/2}$ (where the extinction coefficient, g, was refined to a final value of 7.0 × 10^{-8}), isotropic thermal parameters for the five fixed cyclopentadienyl hydrogen[21] atoms and all cation non-hydrogen atoms converged to $R_1 = 0.065$ and $R_2 = 0.074$ for 2927 independent reflections having $2\theta_{\text{Mo K}\bar{\alpha}} \leqslant 50.7°$ and $I > 3\sigma(I)$. Similar cycles of empirically weighted[23] full-matrix least squares gave final[16] R_1 and R_2 values of 0.065 and 0.077, respectively, for 2927 reflections. All structure factor calculations employed recent tabulations of atomic form factors[17b] and anomalous dispersion corrections[17c] to the scattering factors of the Mo, Ti, and Cl atoms.

All calculations were performed on an IBM 360/65 or IBM 370/158 computer using the following programs: MAGTAPE, SCALEUP, and SCTFT4, data reduction programs written in this laboratory by V. W. Day; FAME, a Wilson plot and normalized structure factor program by R. Dewar and A Stone; MULTAN, a direct methods program, a modified version of Main, Germain, and Woolfson's program; FORDAP, Fourier and Patterson synthesis program, a modified version of A. Zalkin's program; ORFLSE, full-matrix least-squares refinement program, a highly modified version of Busing, Martin, and Levy's original ORFLS; ORFFE, bond lengths and angles with standard deviations by Busing, Martin, and Levy; ORTEP2, thermal ellipsoid plotting program by C. Johnson; MPLANE, least-squares mean plane calculation program from L. Dahl's group.

Results and Discussion

Synthesis and Characterization. The molybdenum complex $[(\eta^5\text{-}C_5H_5)Ti(Mo_5O_{18})][(n\text{-}C_4H_9)_4N]_3$ (**1**) is prepared in CH_2Cl_2 according to eq 1. Its tungsten analogue, $[(\eta^5\text{-}C_5H_5)Ti(W_5O_{18})][(n\text{-}C_4H_9)_4N]_3$ (**2**), cannot be prepared in an analogous fashion since the ditungstate anion is unknown. Compound **2** is therefore prepared in CH_3CN from acidified monotungstate anion:

$$5Mo_2O_7^{2-} + 2(C_5H_5)_2TiCl_2 + H_2O \rightarrow 2[(C_5H_5)Ti(Mo_5O_{18})]^{3-} + 2C_5H_6 + 4Cl^- \quad (1)$$

$$5WO_4^{2-} + 5H^+ + (C_5H_5)_2TiCl_2 \rightarrow [(C_5H_5)Ti(W_5O_{18})]^{3-} + C_5H_6 + 2Cl^- + 2H_2O \quad (2)$$

Both compounds **1** and **2** can be obtained as analytically pure, crystalline materials in moderate yields (60% for **1**, 40% for **2**). As expected for isostructural species, their IR spectra are extremely similar in the 350–1000-cm^{-1} region (see Figure 1). The tungsten compound is very stable toward hydrolysis and can, for example, be refluxed in a 1:2 volume:volume mixture of H_2O and CH_3CN for at least 3 h without decomposition detectable by IR or NMR spectroscopy. The molybdenum compound, however, is moisture sensitive and decomposes completely under the same conditions in less than 1 h.

^{17}O NMR Spectra. Compounds **1** and **2** display completely resolved ^{17}O NMR spectra shown in Figure 2 which are easily assigned to chemically nonequivalent oxygen types by comparison with chemical shift data for $M_6O_{19}^{2-}$ and $VM_5O_{19}^{3-}$, M = Mo, W.[14] Resonances for the two nonequivalent OM terminal oxygens (O_E and O_F in Figure 2) can be assigned with use of intensity arguments. Resonances for the two nonequivalent bridging OM_2 oxygens (O_B and O_C in Figure 2), however, have equal intensities and cannot be uniquely assigned to specific oxygens.

Several workers have noted crude correlations between ^{17}O chemical shifts in oxomolybdenum(VI) units and Mo^{VI}–O bond lengths, bond strengths, and/or oxygen charge.[13b,14,24-27] When a given Mo–O bond is weakened, implying a longer bond and more negative charge on the oxygen, the chemical shift for the oxygen in question is displaced upfield. Here, for example, the OMo terminal oxygen resonances for the $[(\eta^5\text{-}C_5H_5)Ti(Mo_5O_{18})]^{3-}$ trianion appear 99 and 70 ppm upfield relative to the 933 ppm[14] resonances for terminal oxygens in the $Mo_6O_{19}^{2-}$ dianion. Curiously, the chemical shift for the unique OMo terminal oxygen

---

[16] See paragraph at end of paper regarding supplementary material.

[17] "International Tables for X-ray Crystallography"; Kynoch Press: Birmingham, England, 1974; Vol. IV: (a) pp 55–66; (b) pp 99–101; (c) pp 149–50.

[18] "International Tables for X-ray crystallography"; Kynoch Press: Birmingham, England, 1969; Vol. I, p 200.

[19] "International Tables for X-ray Crystallography"; Kynoch Press: Birmingham, England, 1967; Vol. II, p 302.

[20] The R values are defined as $R_1 = \sum||F_o| - |F_c||/\sum|F_o|$ and $R_2 = [\sum w(|F_o| - |F_C|)^2/\sum w|F_o|^2]^{1/2}$, where w is the weight given each reflection. The function minimized is $\sum w(|F_o| - K|F_c|)^2$, where K is the scale factor.

[21] The following idealized atomic coordinates were calculated for the five cyclopentadienyl hydrogen atoms assuming sp^2 hybridization of the respective ring carbon and a C–H bond length of 0.95 Å: H_1, 0.0662, 0.3662, 0.1322; H_2, 0.1065, 0.3250, 0.0922; H_3, 0.1961, 0.3591, 0.0868; H_4, 0.2097, 0.4370, 0.1181; H_5, 0.1259, 0.4385, 0.1453. These hydrogen atoms were assigned isotropic thermal parameters of 10.0 Å^2 and were not allowed to vary in refinement cycles.

[22] Zachariasen, W. H. *Acta Crystallogr.* **1967**, *23*, 558–64.

[23] Empirical weights were calculated from the equation $\sigma = \sum_0^3 a_n|F_o|^n = 18.0 - (7.32 \times 10^{-2})F_o + (2.23 \times 10^{-4})|F_o|^2 - (1.30 \times 10^{-7})|F_o|^3$, the a_n being coefficients derived from the least-squares fitting of the curve $||F_o| - |F_c|| = \sum_0^3 a_n|F_o|^n$, where F_c values were calculated from the fully refined model with use of unit weighting and an $I > 3\sigma(I)$ rejection criterion.

[24] Filowitz, M.; Klemperer, W. G.; Messerle, L.; Shum, W. *J. Am. Chem. Soc.* **1976**, *98*, 2345–6.

[25] Miller, K. F.; Wentworth, R. A. D. *Inorg. Chem.* **1979**, *18*, 984–8.

[26] Fedotov, M. A.; Maksimovskaya, R. I.; Molchanova, G. A.; Alyasova, A. K. *Izv. Akad. Nauk SSSR, Ser. Khim.* **1980**, 709–12.

[27] Freeman, M. A.; Schultz, F. A. Reilley, C. N. *Inorg. Chem.* **1982**, *21*, 567–76.

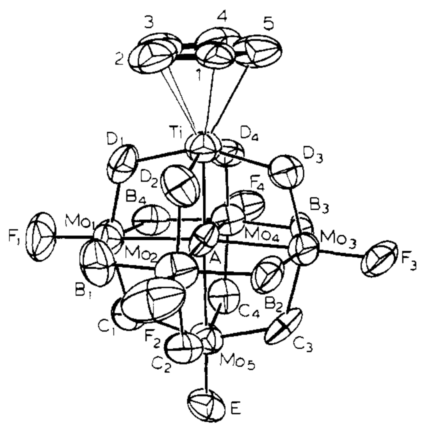

Figure 3. Perspective ORTEP drawing of the solid-state structure for non-hydrogen atoms of the $[(\eta^5\text{-}C_5H_5)Ti(Mo_5O_{18})]^{3-}$ anion as observed in crystalline **1**. All atoms are represented by thermal vibration ellipsoids drawn to encompass 50% of the electron density. Oxygen and carbon atoms are labeled by their subscripts: capital letters and numbers for oxygens and only numbers for carbons.

Chart I

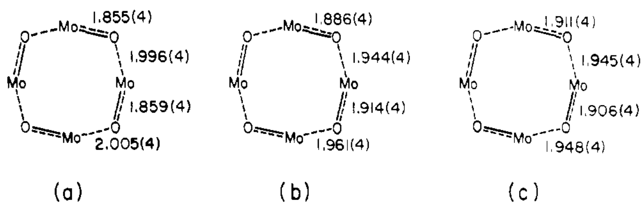

Chart II

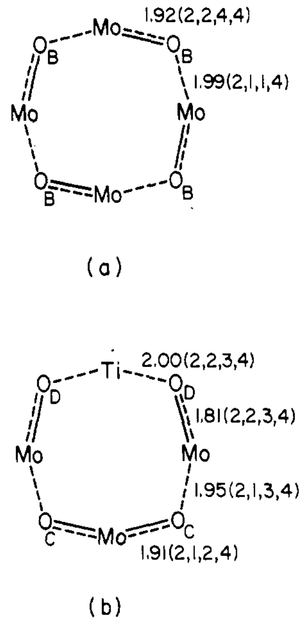

(O_E in Figure 2) lies upfield relative to the chemical shift for the four equivalent OMo terminal oxygens (O_F in Figure 2), even though the O_E oxygen is more remote from the Ti^{IV} center. This implies that the local increase in negative surface charge implied by the replacement of an $[OMo^{VI}]^{4+}$ unit in $Mo_6O_{19}^{2-}$ by a $[(\eta^5\text{-}C_5H_5)Ti^{IV}]^{3+}$ unit to form $[(\eta^5\text{-}C_5H_5)Ti(Mo_5O_{18})]^{3-}$ (see D) is delocalized to the distal O_E oxygen to a greater extent than to a proximal O_F oxygen. Reexpressed in terms of bond strengths, the distal $Mo-O_E$ bond is weakened more than a proximal $Mo-O_F$ bond. An X-ray crystallographic study of **1** was undertaken in an effort to determine the mechanism of this unusual effect.

Solid-State Structure of $[(\eta^5\text{-}C_5H_5)Ti(Mo_5O_{18})][(\textit{n}\text{-}C_4H_9)_4N]_3\cdot CH_2Cl_2$. The X-ray structural analysis established that single crystals of **1** are composed of discrete $(n\text{-}C_4H_9)_4N^+$ cations, CH_2Cl_2 solvent molecules of crystallization, and $[(\eta^5\text{-}C_5H_5)Ti(Mo_5O_{18})]^{3-}$ anions shown in Figure 3. Final atomic coordinates that resulted from this structural analysis are presented with estimated standard deviations in Table II; anisotropic thermal parameters for non-hydrogen atoms of the $[(\eta^5\text{-}C_5H_5)Ti(Mo_5O_{18})]^{3-}$ anion and CH_2Cl_2 solvent molecule are listed in Table III.[16] The numbering scheme used to designate atoms of **1** is shown in Figures 3 and 4.[16]

Since the $[(\eta^5\text{-}C_5H_5)Ti(Mo_5O_{18})]^{3-}$ anion in **1** represents a structural modification of the well-known $Mo_6O_{19}^{2-}$ anion in which one Mo atom and its terminally bonded oxygen have been replaced by a $(\eta^5\text{-}C_5H_5)Ti$ unit, it should be possible to assess the structural and electronic effects of such a substitution by comparing structural parameters for both anions. Of the three $Mo_6O_{19}^{2-}$ salts that have been examined crystallographically,[4] the cyclophosphazene complex[4a] has yielded the most precise structural parameters and will therefore be used in the present comparisons. In this structure (see B), the $Mo-O_t$ terminal oxygen bond lengths do not differ significantly, varying between 1.676 (4) and 1.678 (4) Å, as is the case also for the $Mo-O_c$ central oxygen bond lengths, which vary between 2.312 (4) and 2.324 (4) Å. The $Mo-O_b$ bridging oxygen bond lengths display significant variations, however, ranging between 1.855 (4) and 2.005 (4) Å. These variations are not random, and their systematic nature is evident from inspection of bond lengths in the three sets of mutually perpendicular, coplanar $Mo_4(O_b)_4$ oxomolybdenum rings present in the centrosymmetric $Mo_6O_{19}^{2-}$ structure.[28] These are shown in Chart I, where long single bonds (1.928–2.005 Å) are represented by dashed lines and short single bonds (1.855–1.928 Å) are represented by a solid plus a dashed line; i.e., the structure's 1.928-Å average $Mo-O_b$ bond length is used to categorize long and short single bonds. A pattern of bond length alternation is clearly evident in each oxomolybdenum ring. Note that there is relatively less variation in $O_b\cdots O_b$ distances that range from 2.614 to 2.690 Å. The $Mo-O_b$ bond alternation is therefore best viewed as a case of classical off-center displacement[30] of metals in a relatively rigid, close-packed oxygen framework as opposed to semibridging oxygen ligand behavior in a rigid metal framework.[31] Note also that the degree of bond length alternation in one of the oxomolybdenum rings shown in Chart I differs significantly from that in the other two. If Δ is defined as the difference between average long and short bonds within an oxomolybdenum ring, Δ = 0.144 Å in (a) but only 0.053 Å in (b) and 0.038 Å in (c). At an individual molybdenum center, therefore, bond length alternation occurs predominantly as trans bond alternation. The trans character of this bond alternation is in part a consequence of off-center displacement; if oxygen centers are fixed, displacement of a molybdenum toward one oxygen implies equivalent displacement away from the trans oxygen. Orbital arguments, of course, also favor trans as opposed to cis bond length alternation.

Systematic variation of bond lengths in the $[(\eta^5\text{-}C_5H_5)Ti(Mo_5O_{18})]^{3-}$ structure is more difficult to establish due to the relatively low precision of the structure determination. Trends are apparent, however, from the C_4-averaged bond lengths given in Table IV. Analysis of $M_4(O_b)_4$ rings following the same procedure used for Chart I but using C_4-averaged bond lengths yields Chart II, where single bonds are categorized as short or long relative to the structure's 1.93 (2,5,14,24) Å[29] average $M-O_b$ bond length—a value identical with that observed in $Mo_6O_{19}^{2-}$. In the $Mo_4(O_B)_4$ ring, bond length alternation follows the same

---

(28) See ref 5c for a more complete treatment.

(29) The first number in parentheses following an averaged value of a bond length or angle is the root-mean-square estimated standard deviation of an individual datum. The second and third numbers, when given, are the average and maximum deviations from the averaged value, respectively. The fourth number represents the number of individual measurements that are included in the average value.

(30) Megaw, H. D. *Acta Crystallogr., Sect. B: Struct. Crystallogr. Cryst. Chem.* **1968**, *B24*, 149–53 and references cited therein.

(31) Cotton, F. A.; Wilkinson, G. "Advanced Inorganic Chemistry", 4th ed.; Wiley: New York, *1980*; pp *1057–60*.

Table II. Atomic Coordinates for Non-Hydrogen Atoms in Crystalline $[(\eta^5\text{-}C_5H_5)Ti(Mo_5O_{18})][N(n\text{-}C_4H_9)_4]_3\cdot CH_2Cl_2$[a]

atom type[b]	fractional coordinates			B,[c] Å^2	atom type[b]	fractional coordinates			B,[c] Å^2
	10^4x	10^4y	10^4z			10^4x	10^4y	10^4z	
				Anion					
Mo_1	2695.9 (9)	2422.7 (10)	1389.9 (9)	5.1	O_{D1}	2328 (7)	2946 (8)	1215 (3)	5.4
Mo_2	1500.8 (10)	2108.8 (10)	1600.0 (–)[d]	5.5	O_{D2}	1339 (7)	2655 (8)	1383 (4)	5.7
Mo_3	1561.8 (10)	3060.9 (11)	2045.2 (8)	5.6	O_{D3}	1373 (8)	3451 (7)	1762 (4)	5.5
Mo_4	2755.3 (10)	3381.4 (9)	1835.7 (6)	4.7	O_{D4}	2356 (7)	3719 (6)	1590 (4)	4.7
Mo_5	2504.9 (10)	2152.4 (8)	2022.2 (8)	4.7	O_E	2791 (8)	1715 (7)	2245 (4)	5.3
Ti	1771.8 (20)	3321.7 (19)	1421.4 (11)	4.9	O_{F1}	3130 (9)	2181 (9)	1172 (5)	6.5
O_A	2115 (6)	2763 (6)	1707 (3)	4.0	O_{F2}	1062 (8)	1638 (8)	1537 (5)	7.4
O_{B1}	2092 (8)	1936 (7)	1356 (4)	4.9	O_{F3}	1169 (9)	3264 (9)	2287 (4)	7.5
O_{B2}	1160 (7)	2457 (8)	1893 (4)	6.2	O_{F4}	3226 (7)	3812 (7)	1942 (4)	5.5
O_{B3}	2170 (7)	3499 (6)	2096 (4)	4.7	C_1	992 (13)	3751 (15)	1242 (6)	6.6
O_{B4}	3111 (6)	2996 (6)	1568 (4)	4.3	C_2	1223 (12)	3516 (13)	1029 (6)	5.3
O_{C1}	2887 (7)	2010 (6)	1707 (4)	4.5	C_3	1710 (15)	3718 (12)	994 (6)	6.5
O_{C2}	1924 (8)	1758 (6)	1865 (4)	5.3	C_4	1798 (12)	4141 (14)	1167 (6)	5.9
O_{C3}	1968 (7)	2509 (7)	2224 (4)	6.0	C_5	1331 (15)	4138 (10)	1315 (6)	5.0
O_{C4}	2926 (6)	2778 (6)	2063 (4)	4.4					

atom type[b]	fractional coordinates			B,[c] Å^2	atom type[b]	fractional coordinates			B,[c] Å^2
	10^3x	10^3y	10^3z			10^3x	10^3y	10^3z	
				Cation 1					
N	461 (1)	238 (1)	180 (1)	10 (1)	C_{g1}	518 (3)	100 (3)	192 (1)	17 (2)
C_{a1}	500 (2)	196 (1)	185 (1)	8 (1)	C_{g2}	395 (4)	215 (4)	241 (2)	27 (4)
C_{a2}	411 (2)	235 (2)	199 (1)	11 (1)	C_{g3}	496 (3)	388 (3)	191 (2)	18 (2)
C_{a3}	492 (2)	285 (2)	188 (1)	10 (1)	C_{g4}	460 (3)	220 (3)	102 (2)	20 (2)
C_{a4}	433 (2)	231 (2)	154 (1)	10 (1)	C_{d1}	515 (5)	50 (4)	177 (3)	33 (5)
C_{b1}	475 (2)	141 (3)	178 (1)	15 (2)	C_{d2}	397 (3)	242 (3)	274 (2)	23 (3)
C_{b2}	436 (2)	242 (2)	228 (1)	14 (2)	C_{d3}	469 (4)	425 (4)	208 (2)	29 (4)
C_{b3}	459 (2)	335 (2)	178 (1)	14 (2)	C_{d4}	487 (4)	202 (4)	86 (2)	23 (3)
C_{b4}	482 (2)	241 (2)	130 (1)	13 (1)					
				Cation 2					
N	210 (1)	202 (1)	47 (1)	8 (1)	C_{g1}	343 (2)	280 (2)	53 (1)	13 (1)
C_{a1}	260 (2)	233 (1)	58 (1)	9 (1)	C_{g2}	86 (3)	169 (3)	90 (1)	17 (1)
C_{a2}	175 (2)	195 (2)	70 (1)	13 (1)	C_{g3}	130 (2)	310 (2)	14 (1)	14 (1)
C_{a3}	185 (1)	238 (1)	25 (1)	8 (1)	C_{g4}	278 (4)	66 (4)	29 (2)	10 (2)
C_{a4}	228 (2)	155 (2)	34 (1)	9 (1)	C_{d1}	392 (2)	294 (2)	33 (1)	15 (2)
C_{b1}	304 (2)	247 (2)	39 (1)	12 (1)	C_{d2}	29 (3)	129 (3)	85 (2)	22 (3)
C_{b2}	131 (3)	161 (3)	65 (2)	19 (2)	C_{d3}	107 (3)	363 (3)	16 (2)	19 (2)
C_{b3}	159 (2)	290 (2)	34 (1)	13 (1)	C_{d4}	291 (4)	36 (4)	45 (2)	29 (4)
C_{b4}	261 (3)	119 (3)	52 (1)	18 (2)					
				Cation 3					
N	238 (1)	31 (1)	191 (1)	11 (1)	C_{g1}	349 (3)	–34 (3)	228 (2)	18 (2)
C_{a1}	272 (2)	–12 (2)	201 (1)	13 (1)	C_{g2}	151 (3)	69 (3)	249 (1)	19 (2)
C_{a2}	208 (2)	62 (2)	209 (1)	12 (1)	C_{g3}	335 (3)	88 (3)	138 (1)	15 (2)
C_{a3}	270 (3)	66 (2)	171 (1)	15 (2)	C_{g4}	133 (4)	21 (4)	127 (2)	27 (3)
C_{a4}	207 (2)	5 (2)	170 (1)	12 (1)	C_{d1}	381 (4)	–23 (3)	255 (2)	24 (3)
C_{b1}	310 (3)	8 (3)	218 (1)	15 (2)	C_{d2}	96 (6)	56 (6)	248 (3)	42 (6)
C_{b2}	170 (2)	24 (2)	226 (1)	14 (2)	C_{d3}	372 (4)	72 (4)	117 (2)	24 (3)
C_{b3}	291 (4)	45 (4)	145 (2)	22 (3)	C_{d4}	96 (4)	10 (4)	149 (2)	27 (3)
C_{b4}	166 (3)	37 (3)	158 (2)	18 (2)					
				Solvent					
C	329 (2)	273 (4)	112 (1)	11.2	Cl_2	311 (1)	426 (1)	88 (1)	22.3
Cl_1	396 (1)	374 (1)	109 (1)	20.8					

[a] Figures in parentheses are the estimated standard deviations in the last significant digit. [b] Atoms are labeled in agreement with Figures 3 and 4.[16] [c] B is the equivalent isotropic thermal parameter. For non-hydrogen atoms of the anion and CH_2Cl_2 solvent of crystallization, which are modeled with anisotropic thermal parameters of the form $\exp[-(\beta_{11}h^2 + \beta_{22}k^2 + \beta_{33}l^2 + 2\beta_{12}hk + 2\beta_{13}hl + 2\beta_{23}kl]$, this is the equivalent isotropic thermal parameter calculated from $B = 4[V^2 \det(\beta_{ij})]^{1/3}$; for atoms of the cations, this is the isotropic temperature factor that was actually refined. [d] Mo_2 was used to define the origin of the unit cell along $\vec{c}$. This is therefore a symmetry-required value and is listed without an estimated standard deviation.

pattern observed in Chart I. This pattern is not found in the $TiMo_3O_4$ rings. The pattern observed, however, is systematic and is a direct consequence of replacing a tetravalent $[Mo^{VI}O_t]^{4+}$ unit (see A) with a trivalent $[Ti^{IV}(C_5H_5)]^{3+}$ unit (see D). Since the Ti–O_D bonds are weaker than Mo–O single bonds, the Mo_g–O_D[32] bonds are short, and the Mo_g–O_C[32] bonds trans to them are weakened. This in turn leads to a shortening of the Mo_5–O_C bonds. Since all four Mo_5–O_C bonds are shortened, constant valence at Mo_5 can be approximated only if the Mo_5–O_t and/or Mo_5–O_A bonds are weakened. Both are in fact longer than their Mo_g[32] counterparts: $d_{Mo_5-O_E} = 1.73\ (2)$ Å, $d_{Mo_g-O_F} = 1.66\ (2,1,3,4)$ Å,[29] $d_{Mo_5-O_A} = 2.42\ (2)$ Å, $d_{Mo_g-O_A} = 2.33\ (2,0,0,4)$ Å. A trans bond length alternation mechanism can therefore account for the charge delocalization scheme suggested by the ^{17}O NMR data discussed above.

The pattern of bond length alternation observed in $[(\eta^5\text{-}C_5H_5)Ti(Mo_5O_{18})]^{3-}$ induced by substitution (see Chart IIb) is also present in the $[M^{IV}(W_5O_{18})_2]^{8-}$ structures, M = Ce,[33] U[34]

---

(32) The four "girdle" molybdenum atoms (Mo_1, Mo_2, Mo_3, and Mo_4) are collectively referred to as Mo_g atoms.

(33) Iball, J.; Low, J. N.; Weakley, T. J. R. *J. Chem. Soc., Dalton Trans.* **1974**, 2021–4.

Table IV. Bond Lengths (Å) and Angles (deg) in the $[(\eta^5\text{-}C_5H_5)TiMo_5O_{18}]^{3-}$ Anion in Crystalline $[(\eta^5\text{-}C_5H_5)TiMo_5O_{18}][N(n\text{-}C_4H_9)_4]_3$ (1)[a]

param[b]	value	av[c]	param[b]	value	av[c]	param[b]	value	av[c]	param[b]	value	av[c]
						Lengths					
$Ti-C_1$	2.41 (3)	2.42 (3,2,4,5)	$Ti-O_{D1}$	1.99 (2)	2.00 (2,2,3,4)	Mo_5-O_{C1}	1.89 (2)	1.91 (2,1,2,4)	$Ti\cdots Mo_1$	3.250 (5)	3.250 (5,3,7,4)
$Ti-C_2$	2.46 (3)		$Ti-O_{D2}$	2.01 (2)		Mo_5-O_{C2}	1.93 (2)		$Ti\cdots Mo_2$	3.253 (5)	
$Ti-C_3$	2.38 (3)		$Ti-O_{D3}$	2.01 (2)		Mo_5-O_{C3}	1.91 (2)		$Ti\cdots Mo_3$	3.253 (5)	
$Ti-C_4$	2.43 (3)		$Ti-O_{D4}$	1.97 (2)		Mo_5-O_{C4}	1.91 (2)		$Ti\cdots Mo_4$	3.243 (6)	
$Ti-C_5$	2.40 (3)		Mo_1-O_{D1}	1.84 (2)	1.81 (2,2,3,4)	$Ti-O_A$	2.19 (2)		$Mo_5\cdots Mo_1$	3.293 (6)	3.297 (4,4,8,4)
$Ti-C_g$[d]	2.12 (-)		Mo_2-O_{D2}	1.80 (2)		Mo_1-O_A	2.33 (2)	2.33 (2,0,1,4)	$Mo_5\cdots Mo_2$	3.305 (4)	
Mo_1-O_{B1}	1.96 (2)	1.92 (2,2,4,4)	Mo_3-O_{D3}	1.79 (2)		Mo_2-O_A	2.32 (2)		$Mo_5\cdots Mo_3$	3.297 (4)	
Mo_2-O_{B2}	1.92 (2)		Mo_4-O_{D4}	1.81 (2)		Mo_3-O_A	2.33 (2)		$Mo_5\cdots Mo_4$	3.293 (3)	
Mo_3-O_{B3}	1.90 (2)		Mo_1-O_{C1}	1.97 (2)	1.95 (2,1,3,4)	Mo_4-O_A	2.33 (2)		$Mo_1\cdots Mo_2$	3.284 (3)	3.288 (4,6,11,4)
Mo_4-O_{B4}	1.89 (2)		Mo_2-O_{C2}	1.92 (2)		Mo_5-O_A	2.42 (2)		$Mo_1\cdots Mo_4$	3.299 (4)	
Mo_2-O_{B1}	1.98 (2)	1.99 (2,1,1,4)	Mo_3-O_{C3}	1.95 (2)		Mo_1-O_{F1}	1.66 (2)	1.66 (2,1,3,4)	$Mo_2\cdots Mo_3$	3.285 (4)	
Mo_3-O_{B2}	1.98 (2)		Mo_4-O_{C4}	1.95 (2)		Mo_2-O_{F2}	1.65 (2)		$Mo_3\cdots Mo_4$	3.284 (4)	
Mo_4-O_{B3}	1.99 (2)		Mo_5-O_E	1.73 (2)		Mo_3-O_{F3}	1.65 (2)				
Mo_1-O_{B4}	1.99 (2)					Mo_4-O_{F4}	1.69 (2)				
						Angles					
$CgTiO_{D1}$[d]	105.2 (-)	104.7 (-,10,14,4)	$O_{C1}Mo_1O_{B4}$	83.6 (7)	84.9 (8,8,13,8)	$O_AMo_1O_{B4}$	75.8 (6)	77.7 (7,8,19,8)	$O_{C1}Mo_1O_{D1}$	153.3 (8)	153.5 (8,3,4,4)
$CgTiO_{D2}$[d]	103.5 (-)		$O_{C1}Mo_1O_{B1}$	85.9 (8)		$O_AMo_1O_{B1}$	78.6 (7)		$O_{C2}Mo_2O_{D2}$	153.7 (8)	
$CgTiO_{D3}$[d]	103.8 (-)		$O_{C2}Mo_2O_{B1}$	85.0 (8)		$O_AMo_2O_{B1}$	78.4 (7)		$O_{C3}Mo_3O_{D3}$	153.8 (8)	
$CgTiO_{D4}$[d]	106.1 (-)		$O_{C2}Mo_2O_{B2}$	85.5 (8)		$O_AMo_2O_{B2}$	78.3 (7)		$O_{C4}Mo_4O_{D4}$	153.1 (8)	
$CgTiO_A$[d]	178.0 (-)		$O_{C3}Mo_3O_{B2}$	84.3 (8)		$O_AMo_3O_{B2}$	77.0 (7)		$O_{C1}Mo_5O_{C3}$	153.4 (8)	152.9 (8,5,5,2)
O_ATiO_{D1}	76.0 (7)	75.4 (7,4,6,4)	$O_{C3}Mo_3O_{B3}$	85.9 (8)		$O_AMo_3O_{B3}$	78.7 (7)		$O_{C2}Mo_5O_{C4}$	152.4 (8)	
O_ATiO_{D2}	75.0 (7)		$O_{C4}Mo_4O_{B3}$	83.8 (7)		$O_AMo_4O_{B3}$	76.9 (6)		TiO_AMo_1	92.0 (6)	92.0 (6,2,4,4)
O_ATiO_{D3}	75.0 (7)		$O_{C4}Mo_4O_{B4}$	85.2 (7)		$O_AMo_4O_{B4}$	77.6 (7)		TiO_AMo_2	92.3 (6)	
O_ATiO_{D4}	75.4 (7)		$O_{D1}Mo_1O_{B4}$	87.8 (8)	89.4 (8,13,16,8)	$O_AMo_1O_{C1}$	77.9 (7)	78.2 (7,1,3,4)	TiO_AMo_3	92.1 (6)	
$O_{D1}TiO_{D2}$	86.2 (8)	86.3 (8,5,8,4)	$O_{D1}Mo_1O_{B1}$	90.9 (8)		$O_AMo_2O_{C2}$	78.2 (7)		TiO_AMo_4	91.6 (6)	
$O_{D1}TiO_{D4}$	86.5 (7)		$O_{D2}Mo_2O_{B1}$	87.8 (8)		$O_AMo_3O_{C3}$	78.2 (7)		$Mo_5O_AMo_1$	87.9 (6)	88.0 (6,2,2,4)
$O_{D2}TiO_{D3}$	87.1 (8)		$O_{D2}Mo_2O_{B2}$	91.0 (8)		$O_AMo_4O_{C4}$	78.3 (6)		$Mo_5O_AMo_2$	88.4 (6)	
$O_{D3}TiO_{D4}$	85.5 (7)		$O_{D3}Mo_3O_{B2}$	88.7 (8)		$O_AMo_1O_{D1}$	75.5 (7)	75.4 (7,3,5,4)	$Mo_5O_AMo_3$	88.0 (6)	
$O_{D1}TiO_{D3}$	151.0 (8)	150.7 (8,3,3,2)	$O_{D3}Mo_3O_{B3}$	90.1 (8)		$O_AMo_2O_{D2}$	75.6 (7)		$Mo_5O_AMo_4$	87.7 (5)	
$O_{D2}TiO_{D4}$	150.4 (8)		$O_{D4}Mo_3O_{B3}$	88.3 (7)		$O_AMo_3O_{D3}$	75.6 (7)		$Mo_1O_AMo_2$	89.9 (6)	89.9 (6,2,2,4)
$O_{F1}Mo_1O_{B4}$	102.5 (9)	102.3 (9,7,21,8)	$O_{D4}Mo_3O_{B4}$	90.9 (8)		$O_AMo_4O_{D4}$	74.9 (7)		$Mo_1O_AMo_4$	90.2 (6)	
$O_{F1}Mo_1O_{B1}$	102.9 (9)		$O_EMo_5O_{C1}$	102.3 (8)	103.5 (8,9,12,4)	$O_AMo_5O_{C1}$	76.9 (7)	76.5 (7,4,9,4)	$Mo_2O_AMo_3$	90.0 (6)	
$O_{F2}Mo_2O_{B1}$	103.1 (9)		$O_EMo_5O_{C2}$	104.6 (8)		$O_AMo_5O_{C2}$	75.6 (7)		$Mo_3O_AMo_4$	89.6 (6)	
$O_{F2}Mo_2O_{B2}$	100.2 (10)		$O_EMo_5O_{C3}$	104.3 (8)		$O_AMo_5O_{C3}$	76.5 (7)		TiO_AMo_5	179.3 (8)	
$O_{F3}Mo_3O_{B2}$	102.6 (10)		$O_EMo_5O_{C4}$	102.9 (8)		$O_AMo_5O_{C4}$	76.9 (6)		$Mo_1O_AMo_3$	175.9 (8)	176.0 (8,1,1,2)
$O_{F3}Mo_3O_{B3}$	101.7 (9)		$O_{C1}Mo_5O_{C2}$	86.7 (8)	86.7 (8,7,13,4)	$TiO_{D1}Mo_1$	116.4 (9)	117.2 (10,5,9,4)	$Mo_2O_AMo_4$	176.1 (8)	
$O_{F4}Mo_4O_{B3}$	102.4 (8)		$O_{C2}Mo_5O_{C3}$	85.7 (8)		$TiO_{D2}Mo_2$	117.1 (10)		$Mo_5O_{C1}Mo_1$	117.3 (9)	117.4 (9,2,4,4)
$O_{F4}Mo_4O_{B4}$	102.9 (8)		$O_{C3}Mo_5O_{C4}$	87.0 (8)		$TiO_{D3}Mo_3$	117.3 (10)		$Mo_5O_{C2}Mo_2$	117.8 (9)	
$O_{F1}Mo_1O_{C1}$	100.6 (9)	100.0 (9,4,9,4)	$O_{C4}Mo_5O_{C1}$	88.0 (8)		$TiO_{D4}Mo_4$	118.1 (9)		$Mo_5O_{C3}Mo_3$	117.3 (9)	
$O_{F2}Mo_2O_{C2}$	100.1 (10)		$O_AMo_1O_{F1}$	177.8 (9)	178.0 (9,6,12,4)	$O_{B4}Mo_1O_{B1}$	153.9 (8)	154.7 (8,9,14,4)	$Mo_5O_{C4}Mo_4$	117.1 (9)	
$O_{F3}Mo_3O_{C3}$	100.1 (10)		$O_AMo_2O_{F2}$	177.7 (9)		$O_{B1}Mo_2O_{B2}$	156.1 (8)		$Mo_1O_{B1}Mo_2$	113.1 (9)	114.8 (9,8,17,4)
$O_{F4}Mo_4O_{C4}$	99.1 (8)		$O_AMo_3O_{F3}$	179.2 (9)		$O_{B2}Mo_3O_{B3}$	155.1 (8)		$Mo_2O_{B2}Mo_3$	114.8 (9)	
			$O_AMo_4O_{F4}$	177.3 (8)		$O_{B3}Mo_4O_{B4}$	153.7 (7)		$Mo_3O_{B3}Mo_4$	114.8 (8)	
			$O_AMo_5O_E$	179.2 (8)					$Mo_4O_{B4}Mo_1$	116.4 (8)	
			$O_{F1}Mo_1O_{D1}$	106.0 (10)	106.2 (10,7,15,4)						
			$O_{F2}Mo_2O_{D2}$	106.2 (10)							
			$O_{F3}Mo_3O_{D3}$	105.1 (10)							
			$O_{F4}Mo_4O_{D4}$	107.7 (8)							

[a] Numbers in parentheses following individual entries are the estimated standard deviation in the last significant digit. [b] Atoms are labeled in agreement with Tables II and III and Figure 3. [c] See ref 29. [d] Cg refers to the center of gravity for the five-carbon ring of the cyclopentadienyl ligand.

(E). Since the Ce^{IV}–O and U^{IV}–O bonds in these complexes are weaker than the Ti^{IV}–O bonds in $[(C_5H_5)Ti(Mo_5O_{18})]^{3-}$, substitution-induced trans bond length alternation in the Ce^{IV} and U^{IV} complexes is more pronounced than in the Ti^{IV} complex (see Chart III).

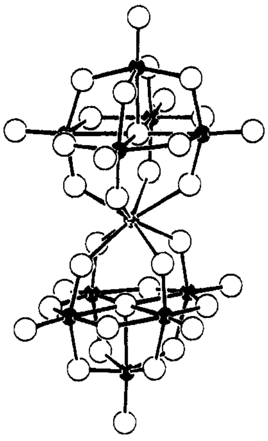

E

Assuming that the response to substitution of $[M^{VI}O_t]^{4+}$ by the lower valent units discussed above can be extended to $M^{VI}{}_6O_{19}{}^{2-}$ derivatives in general, the *trans* bond alternation mechanism can be invoked as an explanation for two general phenomena observed in polyoxohexametalate chemistry. The first, remote activation of polyoxohexametalate surfaces, is exemplified by the approximately equal stabilities of the three $\{[(CH_3)_5C_5]Rh(cis\text{-}Nb_2W_4O_{19})\}^{2-}$ isomers.[9] In each isomer, the Rh^{III} center is bound to three doubly bridging oxygens in the *cis*-$Nb_2W_4O_{19}{}^{4-}$ ligand: one isomer uses three $OW^{VI}{}_2$ oxygens, the second uses one $OW^{VI}{}_2$ and two $OW^{VI}Nb^{V}$ oxygens, and the third uses one $ONb^{V}{}_2$ and two $OW^{VI}Nb^{V}$ oxygens. In the absence of a mechanism for charge delocalization, simple electrostatic considerations dictate that oxygens bonded to Nb^{V} should be more basic than oxygens bonded to W^{VI} and the Rh^{III} should bind preferentially to oxygens bound to pentavalent centers. The absence of such a preference can be explained by trans bond length alternation schemes for charge transmission in $Nb_2W_4O_{19}{}^{4-}$ which delocalize negative charge, helping to avoid electrostatically unfavorable localizations of negative charge. A second general phenomenon that can similarly be explained by trans bond length alternation schemes is the effect of substitution on ^{17}O NMR chemical shifts of remote terminal oxygens in species such as $VW_5O_{19}{}^{3-}$,[14] $VMo_5O_{19}{}^{3-}$,[14] $V_2W_4O_{19}{}^{4-}$,[7] and $Nb_2W_4O_{19}{}^{4-}$.[8,9] Precisely the same effects have been discussed above for the $[(\eta^5\text{-}C_5H_5)Ti(Mo_5O_{18})]^{3-}$ anion, and the explanation outlined there can be transferred directly to these other systems.

We note finally the Ti^{IV} coordination geometry. The most striking feature here is the 2.19 (2) Å Ti–O$_A$ central oxygen bond, which is much shorter than the corresponding 2.319 (4,4,7,3) Å Mo–O$_C$ central oxygen bond length in $Mo_6O_{19}{}^{2-}$. This may arise in part from the weak Mo$_5$–O$_A$ bond (see above) but could also arise from the availability of a 3d$_{z^2}$ Ti orbital which does not interact strongly with the C_5H_5 ring.[35] In $Mo_6O_{19}{}^{2-}$, the corresponding 4d$_{z^2}$ Mo orbital interacts strongly with the O$_t$ terminal oxygen (see A) and is therefore less available for O$_C$ central oxygen bonding. The 2.00 (2,2,3,4) Å Ti–O$_D$ average bond length is comparable to the 1.97-Å Ti–O average distance observed in $(C_5H_5)_6Ti_6O_8$;[36] the 2.42 (3,2,4,5) Å Ti–C average distance is also unexceptional.[37]

Chart III

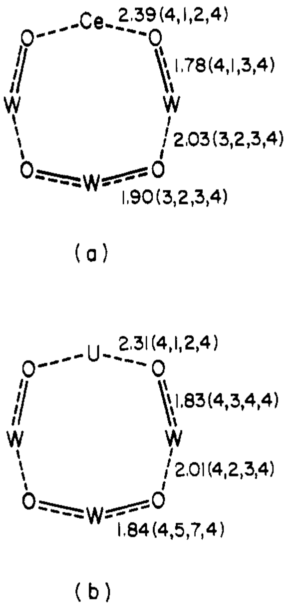

Acknowledgment. W.G.K. acknowledges the National Science Foundation for partial support of the research. Acknowledgment is also made to the University of Illinois NSF Regional NMR Facility (Grant CHE 79-16100). We are also grateful to Dr. Egbert Keller for providing a copy of his SCHAKAL program and Suzanne M. Moenter for preparing the SCHAKAL drawings. Daniel Speiser was instrumental in developing the $(WO_4)[(n\text{-}C_4H_9)_4N]_2$ preparation. Dr. Charles Besecker is responsible for many details of the preparation of compound **1**. Dr. Jenny Green explained to us the nature of bonding at Ti in compound **1**.

Registry No. **1**, 71344-02-0; **1**·CH_2Cl_2, 98576-56-8; **2**, 98576-55-7; $(\alpha\text{-}Mo_8O_{26})[(n\text{-}C_4H_9)_4N]_4$, 59054-50-1; $(Mo_2O_7)[(n\text{-}C_4H_9)_4N]_2$, 64444-05-9; $(C_5H_5)_2TiCl_2$, 1271-19-8; WO_3, 1314-35-8; $(WO_4)[(n\text{-}C_4H_9)_4N]_2$, 60619-93-4.

Supplementary Material Available: Crystal structure analysis report, anisotropic thermal parameters (Table III), bond lengths and angles in the cations and solvent molecule (Table V), ORTEP drawings of cations (Figure 4), and a listing of structure factors for $[(\eta^5\text{-}C_5H_5)TiMo_5O_{18}][(n\text{-}C_4H_9)_4N]_3\cdot CH_2Cl_2$ (29 pages). Ordering information is given on any current masthead page.

---

(34) Golubev, A. M.; Murandyan, L. A.; Kazanskii, L. P.; Torchenkova, E. A.; Simonov, V. I.; Spitsyn, V. I. *Sov. J. Coord. Chem.* (*Engl. Transl.*) **1977**, *3*, 715–20.

(35) Clack, D. W.; Warren, K. D. *Struct. Bonding* (*Berlin*) **1980**, *39*, 1–41.

(36) Huffman, J. C.; Stone, J. G.; Krussell, W. C.; Caulton, K. G. *J. Am. Chem. Soc.* **1977**, *99*, 5829–31.

(37) Steffen, W. L.; Chun, H. K.; Fay, R. C. *Inorg. Chem.* **1978**, *17*, 3498–3503 and references cited therein.